Nov 7th, 12:00 AM - Nov 8th, 12:00 AM

New Proposals for the Direct Strength Method of Design of Cold-Formed Steel Beams with Holes in Shear

Song Hong Pham

Cao Hung Pham

Colin A. Rogers

Gregory J. Hancock

Wei-Wen Yu International Specialty Conference on Cold-Formed Steel Structures
St. Louis, Missouri, U.S.A., November 7 & 8, 2018

New Proposals for the Direct Strength Method of Design of Cold-formed Steel Beams with Holes in Shear

Song Hong Pham[1], Cao Hung Pham[2], Colin A. Rogers[3] and Gregory J Hancock[4]

Abstract

In the latest North American Specification for the design of cold-formed steel structural members AISI S100-16, an empirical approach is specified to design beams with web holes in shear. Recently, a Direct Strength Method (DSM) of design for shear for perforated beams with the aspect ratio (shear span / web depth) of *1.0* has been proposed. This paper presents a comprehensive review of the proposal and an experimental validation using a test series on beams with the aspect ratio of *2.0* and with various square and circular web opening sizes conducted at the University of Sydney, and other experimental data collected from the literature. As a result, it is proven that the earlier proposal reliably predicts the shear strength of perforated structures with centrally located square and circular web holes and with an aspect ratio up to *2.0*.

[1] Doctoral Candidate, School of Civil Engineering, The University of Sydney, NSW 2006, Australia. E-mail: songhong.pham@sydney.edu.au.

[2] Senior lecturer in Structural Engineering, School of Civil Engineering, The University of Sydney, NSW 2006, Australia.
E-mail: caohung.pham@sydney.edu.au.

[3] Associate Professor, Department of Civil Engineering and Applied Mechanics, McGill University, Canada. E-mail: colin.rogers@mcgill.ca

[4] Emeritus Professor and Professorial Research Fellow, School of Civil Engineering, The University of Sydney, NSW 2006, Australia.
E-mail: gregory.hancock@sydney.edu.au

Introduction and Background

For unperforated members subjected to shear force, the DSM design rules in the AISI S100-16 Section G2.2 (AISI 2016) and the AS/NZS4600:2018 (Standards Australia 2018) allow a direct computation of the shear strength as follows:

For $\lambda_v \leq 0.776$

$$V_n = V_y \tag{1a}$$

For $\lambda_v > 0.776$

$$V_n = \left[1 - 0.15\left(\frac{V_{cr}}{V_y}\right)^{0.4}\right]\left(\frac{V_{cr}}{V_y}\right)^{0.4} V_y \tag{1b}$$

where

$$\lambda_v = \sqrt{\frac{V_y}{V_{cr}}}$$

V_{cr} is elastic shear buckling force of the section,

$$V_{cr} = \frac{k_v \pi^2 E A_w}{12\left(1-v^2\right)\left(\frac{h}{t}\right)^2} \tag{2}$$

k_v is shear buckling coefficient of the whole section assuming an average buckling stress in the web, which is given in Pham and Hancock (2009, 2012a) for plain lipped channels based on the Spline Finite Strip Method (SFSM), h is the depth of the flat portion of the web, t is the thickness of the web, E is Young's modulus of steel, and v is Poisson's ratio of steel.

V_y is the yield shear load of the flat web, $V_y = 0.6F_yA_w$ where A_w is the cross sectional area of the flat web element, F_y is the design yield stress

However, for perforated members in shear, both the AISI S100-16 and the AS/NZS 4600:2018 still adopt an empirical approach based on the experimental research by Shan et al. (1994), Schuster et al. (1995), and Eiler et al. (1997). This method allows the shear strength of structures with web holes to be computed as a product of a strength reduction factor q_s and the shear strength of unperforated members. Keerthan and Mahendran (2014) proposed new empirical equations to determine the shear reduction factors relying on the ratio of the circular web opening depth (D) to the clear web height (d_1). These new design formulae were generated by fitting the test results on members with

circular openings; thus, their application for other perforation shapes requires further interpretation. Nonetheless, the preceding approaches are not in line with the DSM design philosophy, which has been implemented in the design for other resultant actions, i.e., bending, compression (for both perforated and unperforated members), and shear (for unperforated members only). Therefore, a DSM design approach for perforated members in shear is required to unify cold-formed steel structural design.

Recently, Pham et al. (2017a) proposed a DSM approach to design beams with web openings with an aspect ratio of *1.0*. The method allows the DSM rules for unperforated members as per the AISI S100-16 and AS4600:2018 to be used but with modification of the elastic shear buckling load (V_{crh}) and the plastic shear capacity (V_{yh}) to account for the influence of the web holes. The buckling load can be determined by a rational linear elastic buckling analysis using such finite element computer packages as Abaqus, Strand7 or software employed finite strip analysis such as ISFSM (Eccher 2007). For shear spans with an aspect ratio of *1.0*, designers are also able to calculate V_{cr} on the basis of the shear buckling coefficients (k_v) extracted from non-dimensional graphs or fitted equations (Pham 2017). Alternatively, Pham et al. (2017b) generated a database of buckling coefficients for channel sections with different square central web hole sizes and aspect ratios using the finite element package Abaqus (Dassault Systèmes Simulia Corp. 2014). This database was used to derive a simple expression for k_v on the basis of non-dimensional geometrical parameters as follows:

$$k_v = 5.39\frac{h}{a} - 3.33\frac{d_h}{h} - 17.7\frac{L_h}{a} + 11.9\frac{A_o}{A} + 5.27 \quad (3)$$

where a is the length of the shear span; h is the flat web depth; L_h is the width of web opening; d_h is the depth of web opening; A_o is the surface area of the web opening; A is the surface area of the flat web plate. The equation, however, does not consider the influence of the flange width on the shear buckling which is important for sections with narrower flanges. This is not an issue for commercially available cold-formed steel sections in Australia, but it should be addressed as common sections in other parts of the world, for example in the U.S.A, might have relatively narrow flanges.

Pham et al. (2017a) proved that, in terms of buckling capacity, there is a correlation between the circular and square hole dimensions expressed as $d=0.825D$ where d is the square size, and D is the circle diameter. As a result, the shear buckling of beams with circular holes can be determined by transforming the circular shape into a square shape.

Pham et al. (2017a), on the basis of an underlying interpretation of the shear yield load and finite element analyses, proposed a design model for the shear yield load for sections with holes (V_{yh}). The model ranges from the unreduced plastic shear capacity for structures with small holes to the shear yielding capacity derived from a Vierendeel plastic mechanism for members with large web holes as mathematically described by

When $0 < \frac{d_h}{h} \le 0.10$, $V_{yh} = V_y$ (4a)

When $0.10 < \frac{d_h}{h} < 0.60$, $V_{yh} = V_y - 2\left(\frac{d_h}{h} - 0.1\right)\left(V_y - V_{vrd,0.6}\right)$ (4b)

When $\frac{d_h}{h} \ge 0.60$, $V_{yh} = V_{vrd}$ (4c)

where V_{vrd} is determined by Eq. (5); and $V_{vrd,0.6}$ is the value of V_{vrd} computed for the perforated section with the ratio of $d_h/h = 0.6$.

$$V_{vrd} = \frac{4M_{pv}}{L_h} \tag{5}$$

where M_{pv} is the plastic bending capacity of the top (or bottom) segment above (or below) the opening, including the flanges and lips, provided that the hole is centrally located; for cold-formed steel sections, the rounded corners are considered as squares for simplicity; and L_h is the width of the web opening.

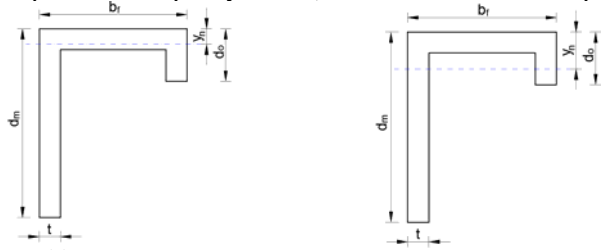

(a) Case 1 (b) Case 2

Figure 1. Location of plastic neutral axis

Figure 1 shows two practical positions of the plastic neutral axis on the top half of a channel section at the location of the web hole. Case 1 corresponds to the neutral axis passing through the top flange with y_n being the distance from the top fibre to the axis, whereas Case 2 is associated with the neutral axis lying below the top flange but it is most likely to cross the lip. The distance y_n is determined as follows:

$$\text{Case 1:}\quad y_n = \frac{t}{2b_f}\left(d_m + d_o - 2t + b_f\right) \le t \tag{6a}$$

$$\text{Case 2:}\quad y_n = 0.25\left(d_m + d_o + 2t - b_f\right) > t \ \text{ and } \ y_n \le d_o \tag{6b}$$

Consequently, the plastic moments corresponding to the two cases are computed as follows:

Case 1:

$$M_{pv} = f_y\left[b_f\frac{y_n^2}{2} + b_f\frac{(t-y_n)^2}{2} + t(d_m - t)\left(\frac{d_m + t}{2} - y_n\right) + t(d_o - t)\left(\frac{d_o + t}{2} - y_n\right)\right] \tag{7a}$$

Case 2:

$$M_{pv} = f_y t\left[(b_f - 2t)\left(y_n - \frac{t}{2}\right) + d_o\left(\frac{d_o}{2} - y_n\right) + d_m\left(\frac{d_m}{2} - y_n\right)\right] \tag{7b}$$

The DSM of design with the modified V_{crh} and V_{yh} determined as above was validated against the experiments on channel section beams with square and circular openings and with an aspect ratio of *1.0* (Keerthan and Mahendran 2013; Pham et al. 2014; Pham et al. 2016). It was found that the proposal reliably predicted the shear strength of those perforated sections. However, its applicability has been restricted to shear spans with an aspect ratio of *1.0*. Further, the experiments as mentioned used a central point load test rig which generated a constant shear force along the shear span and a single curvature bending moment gradient. As discussed in greater detail in Pham et al. (2018), this moment gradient does not affect the shear strength of beams with an aspect ratio of *1.0*. For longer shear panels, however, a substantial strength reduction occurs due to bending effects. Therefore, a more appropriate testing apparatus, referred to as the dual actuator test rig, was developed and validated (Pham et al. 2018). The new test rig was able to minimize the applied bending moments along the shear span, thus enabling the shear strength of beams with an aspect ratio of *2.0* close to pure shear to be achieved. Further details regarding this test rig can be found in the above-mentioned reference.

This paper introduces a test series on high strength cold-formed steel beams with an aspect ratio of *2.0* and with various square and circular web holes using the dual actuator test rig. The experimental results are used to validate and extend the DSM proposal of shear design for structures with web holes as mentioned previously. Further, a revised equation to determine the shear buckling coefficients (k_v) including the influence of the flange width is also presented.

Test Configuration

A detailed description of the test configuration can be found in Pham et al. (2018), and only a brief description is provided in this paper. Figure 2 shows a schematic diagram of the main features of the test setup. The cantilevered cold-formed steel beam was bolted to a stocky column by a moment connection using high strength M12 bolts on the web and M10 bolts on the flanges.

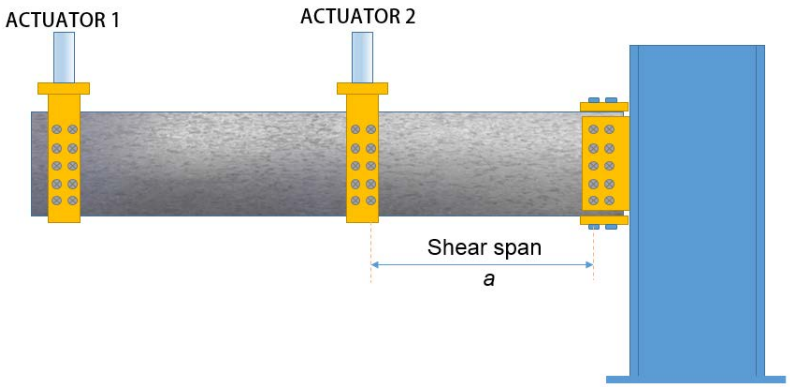

Figure 2. Diagram of the test setup

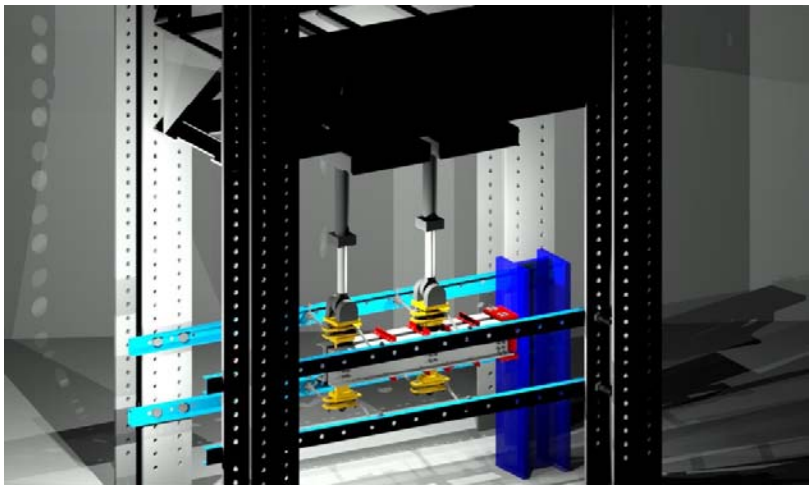

Figure 3. Three dimensional rendered image of the overall test setup

The beam was loaded by two actuators via two *20* mm loading plate assemblies bolted to the beam web. Each MTS actuator has a capacity of *253* kN in compression and *162* kN in tension, and has a stroke of *508* mm. They are controlled simultaneously by an MTS FlexTest® Controller. These actuators are able to move independently with different rates, thus the ratio of the applied moments at the ends of the shear span can be controlled by adjusting these moving rates. In Figure 2, only one channel is shown for clarity. The actual test comprised two channels bolted back to back to the two sides of the loading plates as seen in the 3D rendered Figure 3.

Figure 4 shows an actual test on cold-formed channels with a *145* mm diameter circular web hole. The distortion of the flanges of the two C-section beams was prevented by the 30x30x3EA straps screwed to both top and bottom flanges as used by Pham and Hancock (2012b). The verticality of the system was maintained by means of four pairs of turnbuckles as seen in Figure 3 and 4.

Figure 4. Test specimen during loading

Instrumentation and Test Procedure

During the tests, ten linear variable differential transformers (LVDTs) were used to track the deformation and displacements of the specimens. Of these, six were employed to track the vertical displacements along the length of the beam, and two were mounted to the shear panel adjacent to the opening along the diagonal tension band to measure the out-of-plane deformation. The other two LVDTs were used to track the horizontal movement of the column to which the beams

were fixed. Further, two inclinometers were attached to the top flanges of the specimen pair. The locations of the instruments can be seen in Figure 4. Vishay Model 5100B scanners and the Vishay System 5000 StrainSmart software were used to record the measured data.

The primary aim of the test configuration was to minimize the applied bending moments in the shear span, thus allowing a state close to pure shear to be achieved. This was accomplished by maintaining an applied moment ratio of M_C to M_B of *-1.0* where M_C and M_B are the moments at the connection and at the other end of the shear span, respectively. A default moment rate of *0.5* mm/min was used for both actuators at the beginning. The rate was adjusted according to the actual variation of the moments M_C and M_B monitored in real time so that the ratio of M_C/M_B approached *-1.0*.

Test Matrix

The test series on beams with web holes comprised twelve tests on *200* mm deep and *1.5* mm thick G450 lipped channel sections with square and circular web holes and with an aspect ratio of *2.0*. Of these, six tests were performed on channel sections with square hole sizes (d_h) of *40* mm, *80* mm and *120* mm, consistent with the dimensions used by Pham et al. (2014, 2016); and six tests on sections with circular web holes with the diameters (D) of *50* mm, *100* mm and *145* mm. These equivalent square hole sizes were calculated and rounded from the circular diameters using the relation $d_h=0.825D$. This conversion enables the shear design of structures with circular web holes by transforming the circles to the equivalent square openings as discussed in Pham et al. (2017a). The test matrix is summarised in Table 1. A typical test designation of "C20015-S40" is defined as follows

- "C200" indicates a channel section with the web depth of *200* mm,
- "15" indicates the thickness times *10* in mm,
- "S40" indicates a square hole size (d_h) of *40* mm. Alternatively, "C50" indicates a circular hole with the diameter (D) of *50* mm.

The material yield stress (f_y) was measured by tensile coupon tests and the average value is provided in Table 1.

Table 1. Test matrix - Beams with web holes

Test designation	Shear span (mm)	Hole shape	Hole size (d_h, D) (mm)	Equivalent square size (d_{eq}) (mm)	Steel grade	Measured yield stress (f_y) (MPa)	No of tests
C20015-S40	400	Square	40	40	G450	538.9	2
C20015-S80	400	Square	80	80	G450	538.9	2
C20015- S120	400	Square	120	120	G450	538.9	2
C20015-C50	400	Circular	50	41.3	G450	538.9	2
C20015-C100	400	Circular	100	82.5	G450	538.9	2
C20015-C145	400	Circular	145	119.6	G450	538.9	2

Experimental Results

The ultimate shear forces, $V_{n,T}$, of the test series are summarised in Table 2. The average shear strength of tests on the same section, aspect ratio and material but without web holes (Pham et al. 2018), designated as S2-C20015, is included for comparison. Further, the shear test results on similar channel sections with an aspect ratio of *1.0* and with square web holes conducted by Pham et al. (2014) are reproduced in the last two columns.

It is noted that there is a difference in the yield stresses of these two test series. Therefore, the ultimate shear strength is normalised to the shear yield load (V_y) of the corresponding unreduced sections. The equivalent square hole size (d_{eq}) is the actual size of the square hole (d_h) or the value of *0.825D* for the circular hole with a diameter of D; h is the flat web depth. As can be seen, with the inclusion of the web holes, the shear strength reduction varies from approximately *10%* to *70%* when the ratio of the equivalent square hole size to the flat web depth (d_{eq}/h) ranges from *0.21* to *0.63*. In comparison with the aspect ratio of *1.0* tests (Pham et al. 2014), there is little discrepancy between the shear strength of the tests with large web openings regardless of the aspect ratios. The difference is approximately *8.8%* for the *120* mm square holes. This is contrary to the case of beams with smaller openings where the difference in the shear strength is more substantial, approximately *16%* for beams with *40* mm square holes. As a result, it can be concluded that the large aspect ratio has a noticeable influence on the shear strength of structures with relatively small holes. The ratio, however, causes little effect on beams with substantial web holes. This is because the local stresses around the large holes followed by a Vierendeel failure mechanism as discussed in Pham et al. (2017a) govern the overall behaviour of the members.

Further, it can be observed from the normalised shear strength in Table 2 that the strength of beams with circular openings is very close to the strength of beams with corresponding square openings. For instance, the difference is of maximum of circa *5%* for the pair of *80* mm square hole size and *100* mm diameter circular hole. This close agreement proves that, in terms of the shear strength, the circular holes can be transformed into square ones using the relation $d_{eq} = 0.825D$.

Table 2. Experimental results

Designation	Shear span (mm)	Hole Size (d_h, D) (mm)	d_{eq}/h	Test Series - AR 2.0		Pham et al.(2014)-AR 1.0	
				$V_{n,T}$ (kN)	$V_{n,T}$ /V_y	$V_{n,T}$ (kN)	$V_{n,T}$ /V_y
S2-C20015	400	0	0.00	47.6	0.50		
C20015-S40-1	400	40	0.21	42.1	0.44	46.5	0.530
C20015-S40-2	400	40	0.21	42.7	0.45		
C20015-S80-1	400	80	0.42	29.0	0.31	30.0	0.34
C20015-S80-2	400	80	0.42	28.6	0.30		
C20015-S120-1	400	120	0.63	14.8	0.15	14.8	0.170
C20015-S120-2	400	120	0.63	15.2	0.16		
C20015-C50-1	400	50	0.22	41.9	0.44	na	
C20015-C50-2	400	50	0.22	41.8	0.44		
C20015-C100-1	400	100	0.43	27.5	0.29		
C20015-C100-2	400	100	0.43	27.9	0.29		
C20015-C145-1	400	145	0.63	15.0	0.16		
C20015-C145-2	400	145	0.62	15.7	0.17		

Figure 5 shows typical failure mode shapes of the tests on beams with square and circular holes. Diagonal shear bands across the whole shear span occurred for beams with small web openings (*40* mm square hole and *50* mm circular hole), whereas more localised shear bands were observed for beams with substantially large openings (*120* mm square hole and *145* mm circular hole). This indicates that, for the beams with the large web holes, local effects at the areas close to the holes have a significant role in dictating the shear failure bands. The beams with square holes fractured in the direction perpendicular to

the shear bands at the corners of the openings even though the corners are rounded to *5* mm. The fracture, however, occurred after the peaks and thus out of the scope of this study.

(a) Square hole size of *40* mm

(b) Square hole size of *120* mm

(c) Circular hole with a *50* mm diameter

(d) Circular hole with a *145* mm diameter

Figure 5. Shear failure of beams with square and circular web holes

DSM Validation

The DSM shear proposal (Pham et al. 2017a) employed the existing DSM design formulae for unperforated structures described by Eqs. (1) and (2) but with modified shear buckling force (V_{crh}) and with the yield shear load (V_{yh}) reformulated to account for the influence of the web holes. This section provides a revised equation to compute the shear buckling coefficient (k_v), whereas the yield shear load is determined by Eq. (4), followed by a validation of the DSM proposal using the experimental shear strength as presented previously.

Pham et al. (2017b), from a database of shear buckling coefficients (k_v), derived a simple expression for k_v as in Eq. (3) using an artificial neural network Matlab Toolbox®. In this paper, the database was extended to cover more input parameters including the flange width. *768* finite element models with central square web holes as described in Pham et al. (2017b) were constructed and analysed, aided by a customised Matlab code to generate the Abaqus input files, and a Python script to run the eigenbuckling analyses using the Abaqus processor and extract the buckling loads. The models included *200* mm deep channel section beams with aspect ratios of *1.0*, *2.0* and *3.0*; square hole sizes with the d_h/h ratio ranging from *0.1* to 0.8; thicknesses of *1.2*, *1.5*, *2.4* and *3.0*-mm and flange widths of *50*, *60*, *75* and *85*-mm. The buckling coefficients were subsequently back computed, and the database was input to the neural network to generate the following equation to approximate the values of k_v:

$$k_v = 6.15\frac{h}{a} - 3.63\frac{d_h}{h} - 19.58\frac{L_h}{a} + 13.88\frac{A_o}{A} + 0.57\frac{b_f}{h} + 4.86 \quad (8)$$

The experimental results as presented previously are used to validate and the DSM proposal of design for shear. Table 3 summaries the DSM predictions compared with the experimental shear strengths. The shear buckling force (V_{crh}) was determined by buckling analyses using the computer package Abaqus, $V_{n,T}$ is the experimental shear strength of beams with holes and with the aspect ratio of *2.0*, V_{yh} is the yield shear load determined in accordance with Eqs. (4) and (5), $V_{n,DSM}$ is the shear strength predicted by the DSM with the modified V_{crh} and V_{yh}. The ratios of the test results ($V_{n,T}$) to the predicted values ($V_{n,DSM}$) are shown in the last column together with their coefficient of variation (*CoV*) of *3.29%* and a mean value of *0.98*. These prove a reliable and consistent prediction for the proposal.

Table 3. Shear strength of beams with holes with an aspect ratio of 2.0

Designation	Shear span (mm)	Hole Size (mm)	$V_{n,T}$ (kN)	V_{crh} (kN)	V_{yh} (kN)	λ_v	$V_{n,DSM}$ (kN)	$V_{n,T}/V_{n,DSM}$
C20015-S40-1	400	40	42.1	20.7	80.7	1.97	42.8	0.98
C20015-S40-2	400	40	42.7	20.2	81.2	2.00	42.6	1.00
C20015-S80-1	400	80	29.0	13.8	54.2	1.98	28.6	1.01
C20015-S80-2	400	80	28.6	13.5	54.4	2.01	28.5	1.00
C20015-S120-1	400	120	14.8	9.3	27.6	1.72	16.1	0.91
C20015-S120-2	400	120	15.2	9.2	27.4	1.72	16.0	0.95
C20015-C50-1	400	50	41.9	20.0	79.9	2.00	42.0	1.00
C20015-C50-2	400	50	41.8	20.5	80.4	1.98	42.5	0.98
C20015-C100-1	400	100	27.5	13.4	52.5	1.98	27.8	0.99
C20015-C100-2	400	100	27.9	13.2	52.7	2.00	27.7	1.01
C20015-C145-1	400	145	15.0	9.2	27.6	1.74	16.1	0.94
C20015-C145-2	400	145	15.7	8.7	27.1	1.76	15.6	1.01
							Mean	0.98
							SD	0.03
							CoV (%)	3.29

The test results are normalised and plotted against the DSM design curve (Eq. 1) as shown in Figure 6. The abscissa depicts the section slenderness (λ_v), whereas the ordinate represents the ratio of the shear test results ($V_{n,T}$) to the modified shear yield load (V_{yh}). In this figure, the experimental results of the members as shown in Table 3 are plotted as the solid circles and solid squares for tests with circular and square web holes, respectively. The test results on perforated beams with the aspect ratio of *1.0* conducted by Pham et al. (2014, 2016) and by Keerthan and Mahendran (2013) are also included as hollow points. The graph clearly indicates that the DSM curve is able to predict well the shear strength of cold-formed steel channel sections with circular and square web holes, and with aspect ratios up to *2.0*. Furthermore, the test results on longer shear spans seem to better follow the curve in comparison with the tests on channels with the aspect ratio of *1.0*. The explanation is based on the fact that the former test series was subjected to a minimal moment gradient, thus the shear strength was consistently close to a pure shear strength.

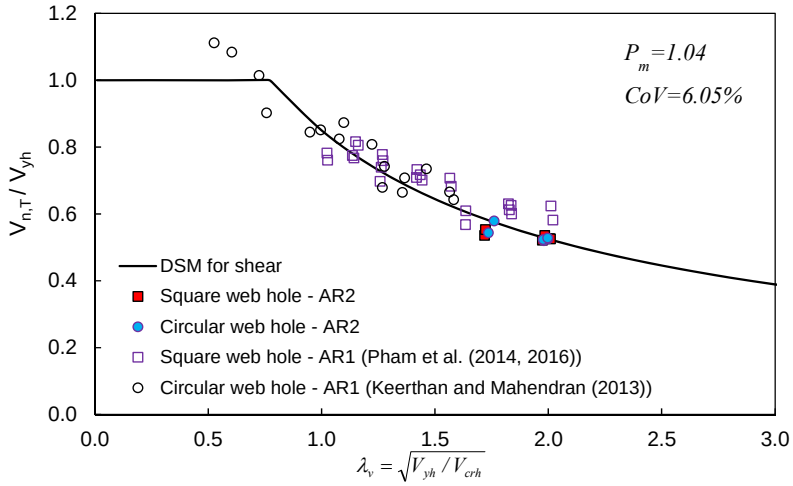

Figure 6. Experimental results in comparison with the DSM shear curve

The mean value and the coefficient of variation of the $V_{n,T}/V_{n,DSM}$ ratios for *30* tests on the perforated beams with the aspect ratio of *1.0* (Pham et al. 2014, 2016; Keerthan and Mahendran 2013) and *12* tests on the perforated beams with the aspect ratio of *2.0* as presented in Table 3 are *1.04* and *6.05%*, respectively.

Comparison with the AISI S100-16

The AISI S100-16 Section G3 allows the shear strength of C-section webs with holes to be determined in accordance with Section G2, with V_{cr} computed using G2.3, multiplied by the strength reduction factor q_s. It is therefore interpreted that Section G2.2 can be used to obtain the shear strength of transversely stiffened beams using the elastic shear buckling force of the flat web alone (not the shear buckling of the full cross-section). Table 4 compares the shear strength obtained by the tests ($V_{n,test}$) and the strength predicted by the AISI S100-16 Section G3 ($V_{n,G3}$). It can be seen that the predictions are close for beams with relatively small web openings. However, for members with large web holes, the AISI provision for shear with holes unexpectedly over-estimates the shear strength, as high as *72%* above the experimental result. Further, the *CoV* of *16.4%* indicates the inconsistency of the prediction.

Table 4. Shear strength predicted by the AISI S100-16 Section G3

Designation	a (mm)	d_h (mm)	t (mm)	h (mm)	$V_{n,test}$ (kN)	q_s	$V_{n,G3}$ (kN)	$V_{n,test}/V_{n,G3}$
C20015-S40-1	400	40	1.54	191.3	42.1	0.91	43.8	0.96
C20015-S40-2	400	40	1.53	191.8	42.7	0.92	43.8	0.98
C20015-S80-1*	400	80	1.54	191.2	29.0	0.67	32.2	0.90
C20015-S80-2*	400	80	1.53	191.7	28.6	0.68	32.2	0.89
C20015-S120-1*	400	120	1.55	191.6	14.8	0.43	20.8	0.71
C20015-S120-2*	400	120	1.54	191.7	15.2	0.43	20.8	0.73
C20015-C50-1	400	50	1.54	191.8	41.9	0.94	45.3	0.92
C20015-C50-2	400	50	1.55	191.2	41.8	0.93	45.3	0.92
C20015-C100-1	400	100	1.55	191.3	27.5	0.72	35.1	0.78
C20015-C100-2	400	100	1.53	191.4	27.9	0.73	34.9	0.80
C20015-C145-1	400	145	1.54	191.4	15.0	0.54	25.8	0.58
C20015-C145-2	400	145	1.50	191.6	15.7	0.55	25.4	0.62
							Mean	0.82
							SD	0.13
							CoV (%)	16.35

Note: * Hole dimensions are out of the limits as per the AISI S100-16 Section G3

Conclusion

The paper presents an experimental program on beams with the aspect ratio of *2.0* and with various square and circular opening sizes using a dual actuator test setup. The new test rig minimized applied bending moments along the shear span, thus allowing a state close to pure shear to be achieved. The experimental shear strength is used to further validate the DSM proposal of shear design for beams with web openings and with aspect ratios up to *2.0*. It was shown that once the shear buckling force and the yield shear load are reformulated to include the influence of the web holes, the existing DSM design rules are capable of predicting reliably the shear strength of perforated structures.

Acknowledgement

Funding provided by the Australian Research Council Discovery Project Grant DP160104640 has been used to perform this project. The first author is supported by the University of Sydney International Scholarship. The authors would like to thank Mr. Minh Toan Huynh, Mr. Dmitry Zelenkin and Mr. Van Bac Mai for their early work on the test rig.

Reference

AISI (2016) North American Specification for the Design of Cold-Formed Steel Structural Members, S100-16th edn. Washington, D.C, U.S.A

Dassault Systèmes Simulia Corp. (2014) Abaqus/CAE, Providence, RI, USA

Eccher G (2007) Isoparametric spline finite strip analysis of perforated thin-walled steel structures. The University of Sydney, Australia; University of Trento, Italy

Eiler M, Laboube R, Yu W (1997) Behavior of web elements with openings subjected to linearly varying shear. Research report, University of Missouri-Rolla, Rolla, Missouri

Keerthan P, Mahendran M (2014) Improved shear design rules for lipped channel beams with web openings. J Constr Steel Res 97:127–142.

Keerthan P, Mahendran M (2013) Experimental studies of the shear behaviour and strength of lipped channel beams with web openings. Thin-Walled Struct 73:131–144

Pham CH (2017) Shear buckling of plates and thin-walled channel sections with holes. J Constr Steel Res 108:800–811. doi: http://dx.doi.org/10.1016/j.jcsr.2016.10.013

Pham CH, Chin YH, Boutros P, Hancock GJ (2014) The behaviour of cold-formed C-sections with square holes in shear. In: 22nd International Specialty Conference on Cold-Formed Steel Structures. St. Louis, Missouri, U.S.A., pp 311–327

Pham CH, Hancock GJ (2009) Shear buckling of thin-walled channel sections. J Constr Steel Res 65:578–585. doi: 10.1016/j.jcsr.2008.05.015

Pham CH, Hancock GJ (2012a) Elastic buckling of cold-formed channel sections in shear. Thin-Walled Struct 61:22–26.

Pham CH, Hancock GJ (2012b) Direct Strength Design of Cold-Formed C-Sections for Shear and Combined Actions. J Struct Eng ASCE 138:759–768. doi: 10.1061/(ASCE)ST.1943-541X.0000510.

Pham CH, Pelosi A, Earls T, Hancock GJ (2016) Experimental and numerical investigations of cold-formed C-sections with square holes in shear. In: 23rd International Specialty Conference on Cold-Formed Steel Structures. Baltimore, U.S.A

Pham SH, Pham CH, Hancock GJ (2017a) Direct Strength Method of Design for Channel Sections in Shear with Square and Circular Web Holes. J Struct Eng 04017017:1–8. doi: 10.1061/(ASCE)ST.1943-541X.0001765

Pham SH, Pham CH, Hancock GJ (2017b) On the Design of Cold-Formed Steel Beams with Holes in Shear Using the Direct Strength Method. In: The 8th European Conference on Steel and Composite Structures

Pham SH, Pham CH, Rogers CA, Hancock GJ (2018) Experimental studies of cold-formed steel beams under uniform shear forces with minimal bending moments. In: Eighth International Conference on THIN-WALLED STRUCTURES, ICTWS 2018. Lisbon, Portugal

Schuster RM, Rogers CA, Celli A (1995) Research into cold-formed steel perforated C-sections in shear. In: Progress Report No. 1 of Phase I of CSSBI/IRAP Project. University of Waterloo Waterloo, Ontario, Canada

Shan M-Y, LaBoube R, Yu W (1994) Behavior of web elements with openings subjected to bending, shear and the combination of bending and shear. Research report, University of Missouri-Rolla, Rolla, Missouri

Standards Australia (2018) AS4600 Cold-formed steel structures. Standards Australian/Standards New Zealand